Kinetic Analysis of Fast Alkalinization Transient by Photoexcited Heterocyclic Compounds: pOH Jump

E. Nachliel, Z. Ophir, and M. Gutman*

Contribution from the Laser Laboratory for fast reactions in Biology, Department of Biochemistry, G.S. Wise Faculty of Life Sciences, Tel Aviv, University of Tel Aviv, Tel Aviv, 69978 Israel. *Received May 20, 1986*

Abstract: Photoexcitation of acridine or 6-methoxyquinoline to their first electronic singlet state is followed by rapid proton abstraction from water, producing the ion pair PhN^*H^+ and OH^-. During the lifetime of the excited state the ions are effectively separated. By the time PhN^*H^+ relaxes to the ground state, the solution is poised in acid–base disequilibrium. The transient deviation of the ground-state reactants from equilibrium is monitored through absorption changes of a pH indicator. Under conditions where the indicator is mostly protonated, pH < pK(In), rapid deprotonation by OH^- is recorded. At pH > pK(In), collisional proton transfer, from $PhNH^+$ to In^-, predominates and the indicator response is transient protonation. The analysis of the results by numerical solution of the coupled nonlinear differential equation yields the diffusion controlled rate constants of all participating reactions.

Excitation of hydroxy aromatic compounds to the first electronic excited singlet state produces a large proton pulse which effectively upset the acid–base equilibrium in theirradiated solution.[1,2] This pH jump method has been employed to measure the diffusion controlled reaction between the proton and various compounds like small molecules in solution,[3] micellar surface,[4] phospholipid membranes,[5] or proteins.[6] On applying this method for the study of enzymes it became apparent that under certain conditions the proton pulse should better be substituted by an OH^- jump.

Heterocyclic compounds excited to the first electronic single state are more basic than their ground state.[7-11] Thus potentially they are suitable for generation of the OH^- pulse. An effective OH^- pulse was demonstrated by Irie,[12] who photodissociated OH^- from triphenylcarbinol. The relaxation in this case was slow (measured in seconds), indicating nondiffusion-controlled steps in the overall reaction.

Recently[10] we employed photoexcitation of 6-methoxyquinoline to record the time-resolved deprotonation of the Halorhodopsin's Schiff base.

In order to introduce this method for quantitative chemical and biochemical studies we have to gain a thorough understanding of the mechanism of the reaction. For this reason we studied the initial step of the perturbation, the reactions during the lifetime of the excited state.[11] We combined steady-state and time-resolved fluorometric measurements to determine the rate constants of proton transfer from solvent to the excited 6-methoxyquinoline (6MQ*) and acridine (AC*). The rate constants were measured in water, in D_2O, and in the presence of high concentrations of monovalent and divalent cations. The results clearly indicated that the mechanism is a proton abstraction from water molecules. The rate of this reaction was grossly enhanced when the H_2O molecule was polarized by the electric field of a nearby cation—like Li^+ (80-fold) Ca^{2+} (200-fold) or Mg^{2+} (330-fold).

In the present study we investigate the events beginning at the end of the photochemical reaction, when the solution is already poised in acid–base equilibrium; both $PhNH^+$ and OH^- concentrations are higher than their equilibrium level.

The formalism we employed for analyzing the results is similar to that used for quantitative analysis of proton pulse.[2] At time zero (in practice about 30 ns after the laser pulse) some PhN molecules have reacted with the solvent water and equal amounts on $PhNH^+$ and OH^- were formed, i.e., $[PhN]_0 = [\widetilde{PhN}] - X_0$, $[PhNH^+]_0 = [\widetilde{PhNH^+}] + X_0$, and $[OH^-]_0 = [\widetilde{OH^-}] + X_0$. ($\bar{C}$ represents the equilibrium concentration.)

The two products $PhNH^+$ and OH^- may react with each other, or with other groups like the indicator molecules (HIn and In^-) presnt in solution.

Scheme I

$$PhN + H^+ \underset{k_2}{\overset{K_1}{\rightleftharpoons}} PhNH^+$$

$$In^- + H^+ \underset{k_4}{\overset{k_3}{\rightleftharpoons}} HIn$$

$$OH^- + H^+ \underset{k_6}{\overset{k_5}{\rightleftharpoons}} H_2O$$

$$OH^- + HIn \underset{k_8}{\overset{k_7^*}{\rightleftharpoons}} In^- + H_2O$$

$$OH^- + PhNH^+ \underset{k_{10}}{\overset{k_9^*}{\rightleftharpoons}} PhN + H_2O$$

$$In^- + PhNH^+ \underset{k_{12}}{\overset{k_4^*}{\rightleftharpoons}} HIn + PhN$$

Collision between OH^- and HIn will lead to alkalinization transient of the indicator. The reaction between $PhNH^+$ and In^- will result in acidification of the indicator ($pK^{In} > pK^{PhNH^+}$). As the incraments of $PhNH^+$ and OH^- are the same, the availability of HIn and In^- will determine whether the perturbation will be observed as acidification or alkalinization of the indicator.

To obtain a precise description of the events we considered all reactions listed in Scheme I (13) and wrote the appropriate differential equations given in the appendix.

The first equation (dX/dt) describes the relaxation of the perturbant (PhN) to its state of equilibrium. The second equation

(1) Gutman, M.; Huppert, D. *Biochem. Biophys. Methods* **1979**, *1*, 9-19.
(2) Gutman, M. *Methods Biochem. Anal.* **1985**, *30*, 1-103.
(3) Gutman, M.; Nachliel, E.; Gershon, E. *Biochemistry* **1985**, *24*, 2937-2941.
(4) Gutman, M.; Nachliel, E.; Gershon, E.; Giniger, R. *Eur. J. Biochem.* **1983**, *154*, 63-39.
(5) Gutman, M.; Nachliel, E.; Fishman, M. *Ion interactions in energy transport systems*; Papageorgio, et al., Eds.; Plenum: New York, 1986; pp 93-105.
(6) Gutman, M. *Methods Enzymol.* **1986**, *127*, 522-538.
(7) Weller, A. *Prog. Reaction Kinetics* **1961**, *1*, 189-214.
(8) Ireland, J. F.; Wyatt, P. A. *Adv. Phys. Org. Chem.* **1976**, *12*, 131-221.
(9) Gafni, A.; Brand, L. *Chem. Phys. Lett.* **1978**, *58*, 346-350.
(10) Gutman, M.; Nachliel, E. *FEBS Lett.* **1985**, *190*, 29-32.
(11) Pines, E.; Huppert, D.; Gutman, M.; Nachliel, E.; Fishman, M. *J. Phys. Chem.* **1986**, *90*, 6366-6370.
(12) Irie, M. *J. Am. Chem. Soc.* **1983**, *105*, 2078-2079.
(13) The thermodynamic favored direction of collisional proton transfer is marked by an asterisk.
(14) Gutman, M.; Huppert, D.; Pines, E. *J. Am. Chem. Soc.* **1981**, *103*, 3709-3713.

0002-7863/87/1509-1342$01.50/0

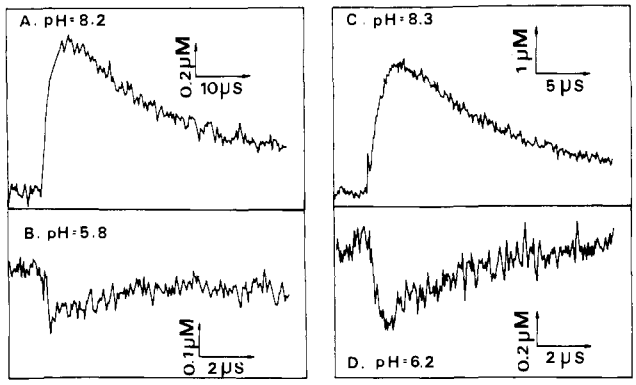

Figure 1. Time-resolved transient absorbance (λ = 633 nm) of bromothymol blue (50 μM) following pulse excitation of either 100 μM acridine (frames A and B) or 1 mM 6-methoxyquinoline (frames C and D). The initial pH of the solution is marked in the frames. Upward deflection corresponds with acidification of the indicator. Each tracing represents a signal accumulated for 512 consecutive laser pulses.

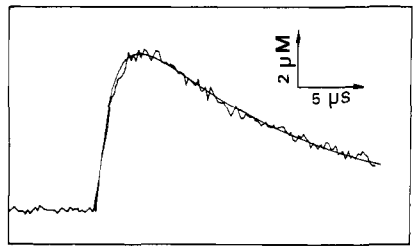

Figure 2. Experimental observation and simulated dynamics of transient protonation of bromothymol blue following pulse excitation of 1 mM 6-methoxyquinoline at pH = 8.0. The simulated curve was generated by solving the differential equations given in the Appendix with the reactant concentrations and the rate constants listed in Tables I, column II. The pulse size was 35 μM of OH^- and PhN^+ generated at $t = 0$. The experimental signal was accumulated for 1024 consecutive laser pulses.

(dY/dt) is for the transient response of the indicator while the last (dZ/dt) corresponds with the change of pH.

In this paper we shall first demonstrate how the experimental results can be analyzed by this formalism and later expand the model to evaluate the role of the various rate constants on the observed dynamics.

Experimental Section

6-Methoxyquinoline and acridine were obtained from Aldrich chemicals and used without further purification.

The excitation pulse of the nitrogen laser (Molectron UV 14) was adjusted by glass filters to the range where the recorded signal was a linear function of the excitation energy.[14] The irradiated solution was placed in a four-face 10 mm × 10 mm quartz cuvette, its contents was constantly mixed, and the pH was monitored during the measurement. Any drift during measurement was corrected by minute addition of NaOH to keep the pH constant (within ± 0.05) during the observation.

Absorbance changes of the solution were monitored by the 633-nm light of a HeNe laser. At this wavelength the extinction coefficient of bromothymol blue is ϵ = 30000 M^{-1} cm^{-1}. The acidic form does not absorb at this wavelength.

The monitoring beam of a HeNe laser was passed perpendicular to the excitation pulse 1 mm behind the front face of the cuvette. Transient absorptions were recorded by a combination of photomultiplier, transient recorder, and averager as described before.[2,5]

Results

The transient absorbance changes of bromothymol blue (50 μM), following laser excitation of a solution containing acridine (0.1 mM) or 6-methoxyquinoline (1 mM), are shown in Figure 1 (A–D). Frames A and B were recorded with acridine at pH 8.2 and 5.8, respectively. At pH 5.8, the ion pair (AcH^+ and OH^-) generated by the pulse led to transient alkalinization of the indicator. At pH 8.2, where the indicator is initially deprotonated, the collisional proton transfer from AcH^+ (pK = 5.3) to the indicator (pK = 7.1) caused a transient acidification. Frames C and D demonstrate the same phenomena with 6-methoxyquinoline instead of acridine.

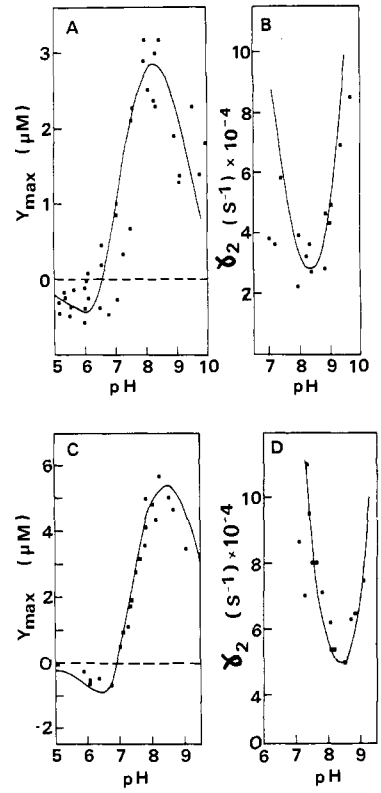

Figure 3. The pH dependence of the amplitude (Y_{max}) and relaxation rate ($\gamma 2$) of the response of bromothymol blue to pulse excitation of 100 μM acridine (A, B) or 1 mM 6-methoxyquinoline (C, D). X_0 = 35 μM. The continuous line are the functions predicted by the solution of the differential equations and the rate constants listed in Table I.

Table I. The Rate Constants of the Partial Reactions Involved in the OH^- Pulse (The Rates Are Defined in Scheme I and Given in $M^{-1}s^{-1}$ Units)

	acridine	6-methoxyquinoline
$k_1(H^+ + PhN)$	$1 \pm 0.1 \times 10^{10}$	$2 \pm 0.15 \times 10^{10}$
$k_3(H^+ + In^-)$	$4.5 \pm 0.1 \times 10^{10}$	$4.5 \pm 0.1 \times 10^{10}$
$k_5(H^+ + OH^-)$	1.2×10^{11}	1.2×10^{11}
$k_7(OH^- + HIn)$	$3.5 \pm 0.15 \times 10^9$ [a]	$3.5 \pm 0.15 \times 10^9$ [a]
$k_9(OH^- + PhNH^+)$	$2.5 \pm 0.20 \times 10^{10}$ [b]	$4 \pm 0.15 \times 10^{10}$
$k_{11}(In^- + PhNH^+)$	$8.5 \pm 0.5 \times 10^9$	$5.25 \pm 0.25 \times 10^9$
$pK_{21}(PhNH)$	5.3	5.0
$pK_{43}(HIn)$	7.1 ± 0.05	7.1 ± 0.05

[a] Compared with 4×10^9.[15] [b] Compared with 1.9×10^{10}.[16]

The differential equations given in the Appendix were solved numerically to reconstruct the observed dynamics of the indicator (for details see ref 2). Figure 2 demonstrates how the computer-generated curve fits the experimental one.

The experiments, described in Figure 1, were repeated over a wide range of initial pH values. The amplitude (Y_{max}) and the rate of signal relaxation (γ_2) of each measurement were determined and drawn as a function of initial pH. Figure 3, frames A and B, depicts the pH dependence of these two macroscopic parameters as measured with acridine. Frames C and D are those recorded with methoxyquinoline. The continuous curves were predicted by the differential equations and the rate constants which simulated a single kinetic experiment as examplified in Figure 2.

The values of all rate constants are listed in Table I.

Discussion

The most striking feature of our measurements is that the very same perturbation causes either acidification or alkalinization of the indicator, as controlled by the initial conditions and its pK. The purpose of our analysis is to extract from these apparently

Scheme II

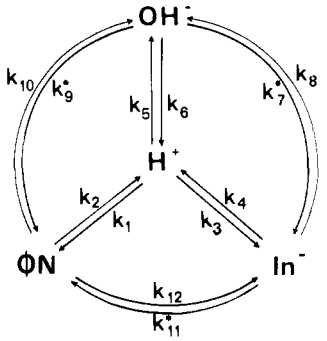

contradicting observations the precise rate constants of the chemical reactions defined in Scheme I.

The analysis is carried out by numerical solution of the differential equations given in the Appendix. Each term in these equations is a product of concentrations and rate constants. The concentrations are measurable parameters. The rate constants are systematically replaced by numerical values. In our search the rate constants are varied within the range of diffusion controlled reactions (10^8–10^{11} M^{-1} s^{-1}). For each combination of rate constants the equations are solved and the computed curve is compared with the experimental one. This search is somewhat simplified by the fact that all equilibrium constants (ratio between forward and backward rate constants) are known and the rate constants (k_3 and k_5) were already determined.[2,6,7,15] Through such repeated iterations a set of rate constants is selected which upon integration reproduces the experimental kinetics (Figure 2). The set is then tested to see if it will also reproduce the dependence of the macroscopic parameters on the initial conditions (see Figure 3). Any set of rate constants which reproduces the observed dynamics whatever the initial conditions (pH, reactants concentration, size of perturbation, etc.) is a legitimate solution of the coupled differential equations. Within the range of diffusion controlled reactions we found only one combination of rate constants which fulfilled these requirements. These rate constants, calculated for acridine and 6-methoxyquinoline, are given in Table I.

The set of rate constants which we accept as the solution of the differential equation is not only self consistant but also concurring with Eigen's previous measurements. The rate of OH^- reaction with cresol red (very similar in structure to bromothymol blue), 4.0×10^9 M^{-1} s^{-1},[15] is very close to the value of $(3.5 \pm 0.15) \times 10^9$ that we measured. Similarly OH^- reaction with acridinium, as determined by Eigen,[16] 1.9×10^{10} M^{-1} s^{-1}, is nearly identical with our value $(2.5 \pm 0.2) \times 10^{10}$.

The transition from alkalinization to acidification of the indicator is accounted for by the differential equations. At pH_0, where the net change of the indicator protonation (defined as Y in the Appendix) is zero, eq 2 in the appendix is grossly simplified. From this expression we obtain the following relationship:

$$pH_0 = pK_{43} - \log [k_7/k_{11} + (K_{21} - K_{43}/X_0)] \quad (1)$$

As the probe is more alkaline than the heterocyclic compound ($K_{21} \gg K_{43}$) we end with the final approximation

$$pH_0 \simeq pK_{43} - \log [k_7/k_{11} + K_{21}/X_0] \quad (2)$$

The pH where the probe will be apparently indifferent of the perturbation is generally close to its pK, in contrast with equilibrium studies where at this range the absorbance changes vs. pH are very large. pH_0 deviates from pK_{43} due to two terms: One is the ratio between the indicator's protonation by $PhNH^+$ (k_{11}) and its deprotonation by OH^- (k_7). The second is the ratio between the perturbant dissociation constant (K_{21}) and the perturbation size (X_0). For the compounds we employed ($pK_{21} \simeq 5$) the ratio

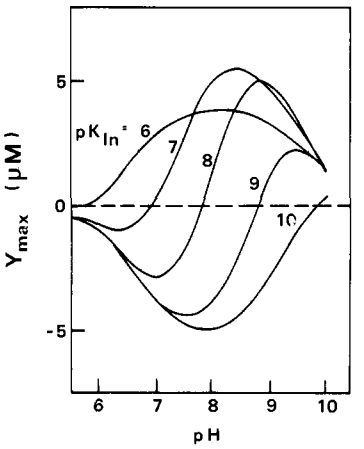

Figure 4. The effect of pH on the amplitude of probes with various pK values. The amplitudes were calculated (as in Figure 3) for systems consisting of 1 mM 6-methoxyquinoline and 50 μM of probes with pK values as indicated in the figure; all other rate constants are those measured for bromothymol blue. The perturbation in all calculations was constant; 35 μM of OH^- and $PhNH^+$ formed at $t = 0$.

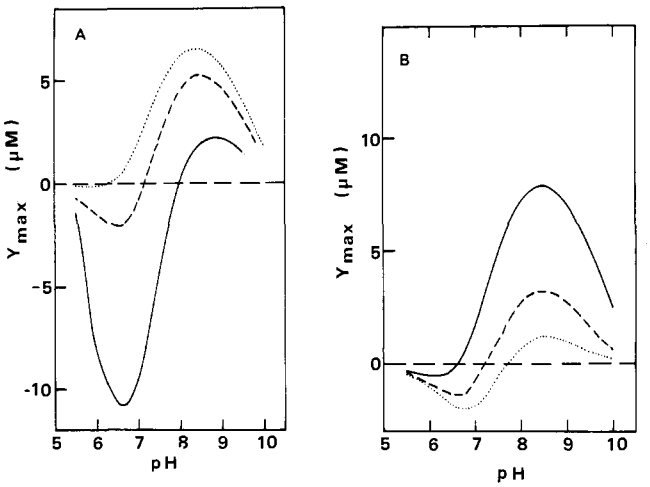

Figure 5. The effect of the rates of collisional proton transfer on the pH dependence of the amplitude. The curves represent the amplitudes of the system consisting of 6-methoxyquinoline (1 mM) and 50 μM probe with pK = 7.0. Frame A depicts the effect of k_7 (deprotonation of probe by OH^-) as it assumes the values 5×10^{10} (—); 7×10^9 (--), and 1×10^9 (···). Frame B depicts the effects of k_{11} (protonation of probe by $PhNH^+$): 1×10^{10} (—), 2.2×10^9 (--), and 5×10^8 (···).

K_{21}/X_0 can vary between 2 (for a weak pulse) and 0.2. Thus low perturbing pulse may cause observable shift of pH_0. In order to obtain large reliable signals it is advisable to carry the experiments 0.5–0.7 pH units above or below the pK and to achieve intensive perturbation.

Figure 4 presents a set of computed curves representing the pH dependence of the amplitude for compounds with different pK values. Acidic compounds (pK = 6) will experience transient acidification whatever the pH. Alkaline compound, at the same pH range, will go to transient deprotonation, while those of intermediate pK will shift from one mode to the other.

The effect of k_7 and k_{11} (see Scheme I and eq 2) on the amplitude is depicted in Figure 5. In Frame A the magnitude of k_7 (rate of HIn reaction with OH^-) was varied between 5×10^{10} and 1×10^9 M^{-1} s^{-1}. The higher rate constant corresponds with diffusion controlled reaction between OH^- and positively charged moiety. The lower one represents a reaction suppressed by strong electrostatic repulsion.[15] Frame B depicts the effect of k_{11} (the collisional protonation of the probe by $PhNH^+$) on the amplitude.

The reconstruction of the observed dynamics (see Figure 2) produces simultaneously the dynamics of all reactants. Figure 6 simulates the transients of $PhNH^+$, OH^-, and HIn as calculated for the experiment depicted in Figure 2. At time zero 35 μM of

(15) Eigen, M.; Kruse, W.; Maasse, G. *Prog. React. Kinet.* **1964**, *2*, 286–318.
(16) Eigen, M. *Angew. Chem., Int. Ed. Engl.* **1964**, *1*, 1–27.

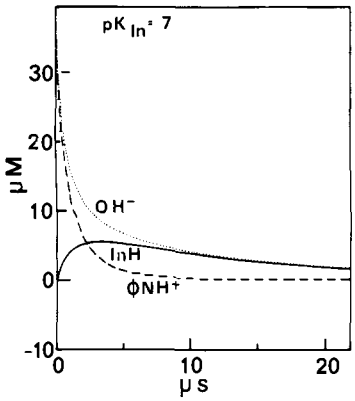

Figure 6. Full kinetic reconstruction of the transient disequilibrium displayed in Figure 2. (—) The dynamics of protonation of the indicator. This curve is identical with the computed fit shown in Figure 2. (···) OH^-; (--) $PhNH^+$.

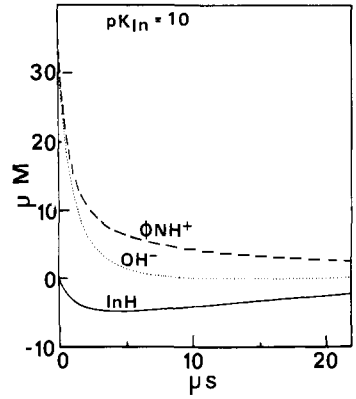

Figure 7. Full kinetic reconstruction of transient disequilibrium in the presence of a probe with pK = 10. The lines are marked as in Figure 6.

OH^- and $PhNH^+$ were formed by the laser pulse. The presence of In^- provides $PhNH^+$ two pathways for relaxations (reaction with OH^- and In^-), while OH^- can relax only by reacting with $PhNH^+$. As a result $PhNH^+$ relaxes more rapidly than OH^-. After 5 μs the disequilibrium is no longer between OH^- and $PhHN^+$ but between OH^- and HIn.

Figure 7 depicts the same scenario for a probe with pK = 10. In this case OH^- relaxes by reaction with $PhNH^+$ and HIn, thus it reaches its prepulse level before $PhNH^+$ and the initial disequilibrium is shifted to the $PhNH^+$ In^- pair. These two figures (Figures 6 and 7) depict how in diffusion controlled system the free energy relationship, through collisional proton transfer, shifts the disequilibrium toward the pair of minimal ΔpK.

The method we described and analyzed is versatile and suitable for measuring proton transfer reactions over a wide range of pH, yet practical limitations are imposed by the pK of the reactants. The implementation of the consideration described above will assist in the selection of experimental conditions where clear analyzable results can be obtained.

Acknowledgment. This research is supported by the American Israel Binational Science Foundation 84/00100.

Appendix

The differential equations describing the transient disequilibrium and its relaxation after incremental formation of $PhNH^+$ (due to proton abstraction from water) are listed below. The rate constants are defined in Scheme I.

X is the increment of OH^- and $PhNH^+$ concentration. Y is the incremental protonation of the indicators and Z corresponds with H^+ concentration which reacted with OH^-. Due to the high concentration of water with respect to all other reactants, H_2O is defined as invariable and its concentration is set as 1.

$$dX/dt = A_{11}X + A_{12}Y + A_{13}Z + B_{11}X^2 + B_{12}XY + B_{13}XZ \quad (A1)$$

$$dY/dt = A_{21}X + A_{22}Y + A_{23}Z + B_{21}Y^2 + B_{22}XY + B_{23}YZ \quad (A2)$$

$$dZ/dt = A_{31}X + A_{32}Y + A_{33}Z + B_{31}Z^2 + B_{32}XZ + B_{33}YZ \quad (A3)$$

where A_{ij} and B_{ij} are defined below.

$$A_{11} = -[k_1(H^+) + k_2 + k_{10} + k_9(PhNH^+) + k_9(OH^-) + k_{12}(HIn) + k_{11}(In^-)]$$

$$A_{12} = -k_9(PhNH^+) + k_{12}(PhN) + k_{11}(PhNH^+)$$

$$A_{13} = -k_1(PhN) + k_9(PhNH^+)$$

$$B_{11} = -k_9;\ B_{12} = -k_9 - k_{12} + k_{11}$$

$$B_{13} = k_1 + k_9$$

$$A_{21} = -k_7(HIn) + k_{11}(In^-) + k_{12}(HIn)$$

$$A_{22} = -[k_3(H^+) + k_4 + k_8 + k_7(HIn) + k_{11}(PhNH^+) + k_{12}(PhN) + k_7(OH^-)]$$

$$A_{23} = -k_3(In^-) + k_7(HIn)$$

$$B_{21} = -k_7;\ B_{22} = -k_7 - k_7 - k_{11} + k_{12}$$

$$B_{23} = k_3 + k_7$$

$$A_{31} = -(k_2 + k_1(H^+) + k_5)$$

$$A_{32} = -k_4 - k_3(H^+) + k_5(H^+)$$

$$A_{33} = -[k_1(PhN) + k_3(In^-) + k_5(OH^-) + k_5(H^+)]$$

$$B_{31} = k_5;\ B_{32} = k_1 - k_5;\ B_{33} = k_3 - k_5$$

Registry No. 6-Methoxyquinoline, 5263-87-6; acridine, 260-94-6.